

CONTROL OF THE RESISTIVE WALL MODE WITH INTERNAL COILS IN THE DIII-D TOKAMAK

by

M. OKABAYASHI, J. BIALEK, A. BONDESON, M.S. CHANCE, M.S. CHU,
D.H. EDGELL, A.M. GAROFALO, R. HATCHER, Y. IN, G.L. JACKSON,
R.J. JAYAKUMAR, T.H. JENSEN, O. KATSURO-HOPKINS, R.J. LA HAYE,
Y.Q. LIU, G.A. NAVRATIL, H. REIMERDES, J.T. SCOVILLE, E.J. STRAIT,
H. TAKAHASHI, M. TAKECHI, A.D. TURNBULL, I.N. BOGATU, P. GOHIL,
J.S. KIM, M.A. MAKOWSKI, J. MANICKAM, AND J. MENARD

NOVEMBER 2004

DISCLAIMER

This report was prepared as an account of work sponsored by an agency of the United States Government. Neither the United States Government nor any agency thereof, nor any of their employees, makes any warranty, express or implied, or assumes any legal liability or responsibility for the accuracy, completeness, or usefulness of any information, apparatus, product, or process disclosed, or represents that its use would not infringe privately owned rights. Reference herein to any specific commercial product, process, or service by trade name, trademark, manufacturer, or otherwise, does not necessarily constitute or imply its endorsement, recommendation, or favoring by the United States Government or any agency thereof. The views and opinions of authors expressed herein do not necessarily state or reflect those of the United States Government or any agency thereof.

CONTROL OF THE RESISTIVE WALL MODE WITH INTERNAL COILS IN THE DIII-D TOKAMAK

by

M. OKABAYASHI,¹ J. BIALEK,² A. BONDESON,³ M.S. CHANCE,¹ M.S. CHU,⁴
D.H. EDGELL,⁵ A.M. GAROFALO,² R. HATCHER,¹ Y. IN,⁵ G.L. JACKSON,⁴
R.J. JAYAKUMAR,⁶ T.H. JENSEN,⁴ O. KATSURO-HOPKINS,² R.J. LA HAYE,⁴
Y.Q. LIU,³ G.A. NAVRATIL,² H. REIMERDES,² J.T. SCOVILLE,⁴ E.J. STRAIT,⁴
H. TAKAHASHI,¹ M. TAKECHI,⁷ A.D. TURNBULL,⁴ I.N. BOGATU,⁵ P. GOHIL,⁴
J.S. KIM, M.A. MAKOWSKI,⁶ J. MANICKAM,¹ AND J. MENARD¹

This is a preprint of a paper to be presented at the 20th IAEA Fusion
Energy Conference, Vilamoura, Portugal, November 1–6, 2004 and to
be published in the *Proceedings*.

¹Princeton Plasma Physics Laboratory, Princeton, New Jersey.

²Columbia University, New York, New York.

³Chalmers University of Technology, Goteborg, Sweden.

⁴General Atomics, P.O. Box 85608, San Diego, California.

⁵Far-Tech, Inc., San Diego, California.

⁶Lawrence Livermore National Laboratory, Livermore, California.

⁷Japan Atomic Energy Research Institute, Naka-machi, Japan.

Work supported by
U.S. Department of Energy
under DE-AC02-76CH03073, DE-FC02-04ER54698, W-7405-ENG-48,
DE-FG02-89ER53297, DE-FG02-03ER83657, and DE-FG03-99ER82791.

GENERAL ATOMICS PROJECT 30200
NOVEMBER 2004

Control of the Resistive Wall Mode With Internal Coils in The DIII-D Tokamak

M. Okabayashi,¹ J. Bialek,² A. Bondeson,³ M.S. Chance,¹ M.S. Chu,⁴ D.H. Edgell,⁵
A.M. Garofalo,² R. Hatcher,¹ Y. In,⁵ G.L. Jackson,⁴ R.J. Jayakumar,⁶ T.H. Jensen,⁴
O. Katsuro-Hopkins,² R.J. La Haye,⁴ Y.Q. Liu,³ G.A. Navratil,² H. Reimerdes,² J.T.
Scoville,⁴ E.J. Strait,⁴ H. Takahashi,¹ M. Takechi,⁷ A.D. Turnbull,⁴ I.N. Bogatu,⁵ P. Gohil,⁴
J.S. Kim,⁵

M.A. Makowski,⁶ J. Manickam,¹ and J. Menard¹

¹Princeton Plasma Physics Laboratory, Princeton, New Jersey, 08543-0451, USA

²Columbia University, New York, New York, USA.

³Chalmers University of Technology, Goteborg, Sweden.

⁴General Atomics, P.O. Box 85608, San Diego, California 92186-5608, USA.

⁵Far-Tech, Inc., San Diego, California 92121, USA.

⁶Lawrence Livermore National Laboratory, Livermore, California, USA.

⁷Japan Atomic Energy Research Institute, Naka-machi, Naka-gun, Ibaraki-ken, 311-0193.

email: mokabaya@pppl.gov

Abstract. New coils were installed inside the vacuum vessel of the DIII-D device for producing non-axisymmetric magnetic fields. These “Internal-Coils” are predicted to stabilize the Resistive Wall Mode (RWM) branch of the long-wavelength external kink mode with plasma beta close to the ideal wall limit. Feedback using these new Internal-Coils was found to be more effective when compared with using the External-Coils located outside the vacuum vessel, because the location inside the vessel allows faster response and their geometry also couples better to the helical mode structure. A proper choice of feedback gain increased the plasma beta above the no-wall limit to $C\beta \geq 0.9$, where $C\beta$ is a measure of achievable beta above no-wall limit defined as $(\beta - \beta_{\text{no-wall.limit}}) / (\beta_{\text{ideal.wall.limit}} - \beta_{\text{no.wall.limit}})$. The feedback system with Internal-Coils can suppress the RWM up to the normalized growth rate $\gamma\tau_w \approx 10$ (τ_w is the resistive flux penetration time of the wall). The feedback-driven dynamic error field correction helps to stabilize the RWM by reducing the rotational drag for $\Omega_{rot} > \Omega_{crit}$, where Ω_{rot} is the angular rotation frequency of plasma and Ω_{crit} is the critical value for the rotational stabilization. When $\Omega_{rot} \sim \Omega_{crit}/2$, the feedback system must stabilize the RWM mainly through direct magnetic control of the mode. The estimated Ω_{crit}/Ω_A is $\approx 2.5\%$ by the MARS-F code analysis with experimentally observed profiles, where Ω_A is the Alfvén angular rotational frequency at $q = 2$ surface. The MARS-F code also predicts that for successful RWM magnetic feedback control the power supply characteristic time should be a fraction of the growth time of the targeted RWM.

1. Introduction

A steady-state, high performance tokamak operation, relying on the self-generated bootstrap current, called Advanced Tokamak [1], is a primary goal of tokamak fusion research aimed at an economically attractive fusion energy source. Both fusion power and bootstrap current are increased with increasing plasma pressure. Ideal MHD theory predicts that a nearby perfectly conducting wall would allow tokamak operation with high pressure plasmas well above the no wall limit. However, due to the finite resistivity of the first wall, these high pressure plasmas can only be sustained for a short period of time before the resistive wall mode (RWM) is excited, leading to plasma pressure collapse. This RWM is characterized by a frequency and growth rate comparable to the inverse of the resistive flux penetration time of the wall, τ_w^{-1} . According to the MHD theory [2–5], the vulnerability of the self-sustained configuration to the long-wavelength ideal external kink can be overcome by plasma rotation and/or magnetic feedback with non-axisymmetric coils assisted by a finite resistance wall. Various codes, such as 2D-, and 3D-MHD codes as well as lumped parameter models, have been developed to assess the feasibility of RWM stabilization [6–10].

In the DIII-D the stabilization experiment with non-axisymmetric coils located outside the vacuum vessel, the “External-coil (C-coils)” [11–13], demonstrated that the RWM can be stabilized by sustained high plasma rotation frequency ($\Omega_{rot} > \Omega_{crit}$) with dynamic error field correction and/or direct magnetic feedback. Here Ω_{rot} and Ω_{crit} are the plasma angular

rotational frequency and the critical angular rotation frequency for the rotational stabilization respectively, both measured at the $q = 2$ surface.

New non-axisymmetric field producing coils, called the “Internal-coils (I-coils)” [14] have been installed inside the DIII-D vacuum and, as we report here, were found to be more effective and efficient when compared with the C-coils located outside the vacuum vessel. With the new I-coils plasma discharges with β_N close to ideal-wall limit have been achieved. The parameter β_N is defined as $\beta/(I_p/aB_t)$, where β is the plasma pressure normalized by the magnetic pressure, a is the plasma minor radius, I_p is the plasma current and B_t is the toroidal field. The poloidal pattern flexibility of I-coil has greatly improved the understanding of the plasma response with the non-axisymmetric fields such as in Resonant Error field Amplification (RFA). In the RFA process, the poloidal mode structure of a weakly stable mode, such as the rotationally stabilized RWM near or above the no-wall limit, responds strongly to the resonant component of an externally applied non-axisymmetric field [15,16]. Recently, application of an active MHD spectroscopy technique has increased the detail knowledge of the RFA process [17].

2. Hardware of Feedback with Internal Feedback Coils (I-coils)

The new internal coils consist of two bands of six coils located above and below the midplane at the outer major radius side as shown schematically in Fig. 1. Each I-coil is a window frame water-cooled single turn coil located 1.5 cm from the vacuum vessel and protected by carbon tiles. Compared with the previous external six C-coils located on the midplane, the internal coils are in close proximity to the plasma surface and, with their more flexible poloidal field structure, prove better at coupling to the RWM. In addition, feedback with the I-coils reduces the phase shift of the feedback field due to the finite impedance of the wall, resulting in a faster time response. More than 50 poloidal field probes and radial flux loops are installed inside and outside the vacuum vessel with analog integrators providing magnetic fields and fluxes rather than the associated time-derivative signals. The feedback logic is provided by a digital control system. In the feedback logic the sensor signals are decomposed to $n=1$ component amplitude and toroidal phase, and the coil currents are energized assuming that the mode remains as a unit body of $n=1$ structure. Effectively the system can be viewed as a single-input and single-output SISO system. The I-coils are designed for up to 7 kA. The feedback coil current is driven by 3.5 kHz switching power amplifiers, for which the maximum current is 5 kA. Based on C-coil experience [11], the internal poloidal field sensors are best suited for the feedback signal, since these probes detect the RWM behavior without vacuum wall shielding as compared to the B_r loops.

2.1. Predicted I-coil Performance with VALEN Code

The VALEN code [7] has been developed to calculate RWM growth rates for configurations which model the complex three-dimensional hardware geometry as realistically as possible. The advantage of internal I-coils is demonstrated as shown in Fig. 2 with the dependence of the growth rate $\gamma\tau_w$ without plasma rotation plotted versus C_β with and without feedback ($\tau_w = 5$ ms is used based on the dominant vacuum vessel eigenvalue), where C_β is a measure of achievable beta above no-wall limit defined as $(\beta - \beta_{\text{no-wall.limit}})/(\beta_{\text{ideal.wall.limit}} - \beta_{\text{no.wall.limit}})$. The feedback power supply is modeled as an ideal

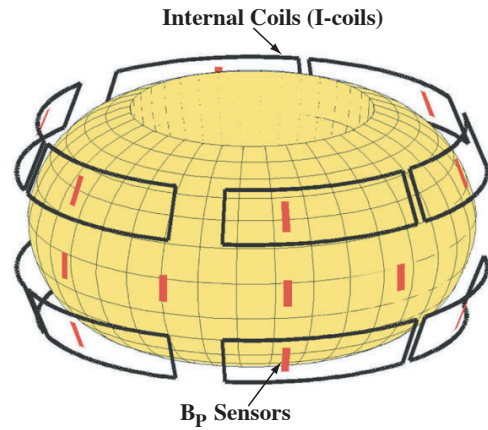


FIG. 1. Schematic diagram of DIII-D magnetic feedback hardware.

voltage source with infinite bandwidth. The coils are controlled using voltage feedback. The model predicts with the new I-coils, the achievable C_β can be drastically improved, approaching the ideal wall limit ($C_\beta > 0.9$). In contrast, the achievable β_N with the previous external C-coils was predicted to be limited to 50% of the ideal wall limit ($C_\beta = 0.5$). The capability of growth rate control with the I-coils is predicted to be improved by more than ten times from $\gamma\tau_w \approx 1.5$ to above 15.

3. Rotational Stabilization at $\Omega_{rot} > \Omega_{crit}$

3.1 Error Field Correction

Recent experiments have revealed several advantages of the internal I-coils. One of them is the optimization of resonant error field compensation by using dynamic error field correction. Dynamic error field correction is a process that utilizes slow feedback operation applied as β_N increases above no-wall limit. The sensors detect the resonantly enhanced amplitude of the rotationally stabilized RWM as it is excited by the error field, and the controller tries to minimize that mode amplitude. In the process, the resultant coil current is the current needed for correcting the component of the error field resonant to a given RWM structure.

The improved error field matching of the poloidal spectrum is made possible by varying the relative connection angle, $\Delta\phi_{connect}$, between the upper and lower I-coils. The current required by the feedback system reaches a minimum with a connection angle of $\Delta\phi_{connect} = 240^\circ - 300^\circ$, due to the better coupling between the RWM structure with the externally applied field [14]. The optimized connection angle around $\Delta\phi_{connect} = 240^\circ - 300^\circ$ [Fig. 3(a)] is consistent with predictions for optimal coupling to the RWM [Fig. 3(b)], made with VALEN, NMA, and MARS codes [10,18,19]

3.2 Rotational Stabilization

In the high rotation regime ($\Omega_{rot} > \Omega_{crit}$), the effect of rotational stabilization can be demonstrated by turning off the feedback process for a short time period. The discharge shown in Fig. 4 is a $C_\beta \approx 0.4$ plasma with large plasma current ramp which creates a plasma configuration above the no-wall limit requiring only modest neutral beam heating power. The main error field correction was made by the external C-coils while the I-coils are used to provide RWM feedback stabilization as well as further fine tuning of the error field

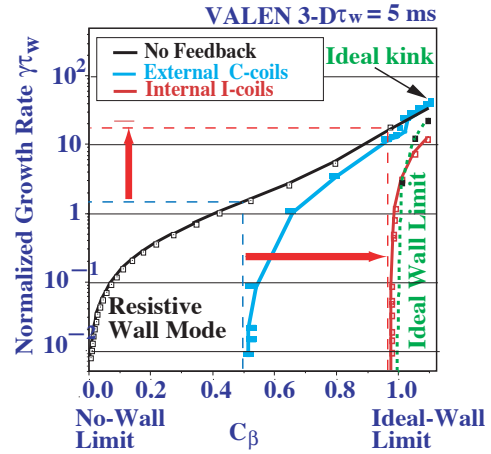


FIG. 2. VALEN code prediction of growth rate without plasma rotation versus C_β with and without feedback (τ_w is 5 ms based on the vacuum vessel eigenvalue).

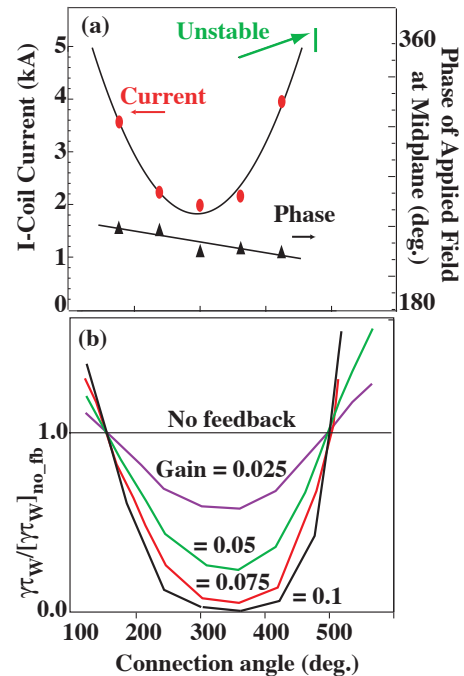


FIG. 3. (a) I-coils current magnitude and toroidal phase of feedback versus connection angle $\Delta\phi_{connect}$ between upper and lower coils (b) The MARS prediction for the feedback growth rate versus connection angle $\Delta\phi_{connect}$ (the gain is unnormalized).

correction. Feedback with the I-coils was initiated at 1300 ms. The discharge initially started with the plasma rotation $\Omega_{rot}/\Omega_A \approx 2\%$ and $C_\beta \approx 0.3-0.4$ (Ω_A is defined as the Alfvénic velocity divided by the major radius at the $q = 2$ surface). The relatively quiet period at relatively high Ω_{rot}/Ω_A around 1300–1400 ms represents the phase of rotational stabilization. To examine the stabilization status, the feedback was turned off at 1350 ms for 10 ms. The plasma response was minimal with an increase in $n=1$ amplitude of less than 5 G on the B_p sensors, showing that at this time in the discharge the rotation is sufficient to stabilize the RWM. Feedback-controlled error field correction with the I-coils has sustained discharges above the no-wall limit for more than one second [14].

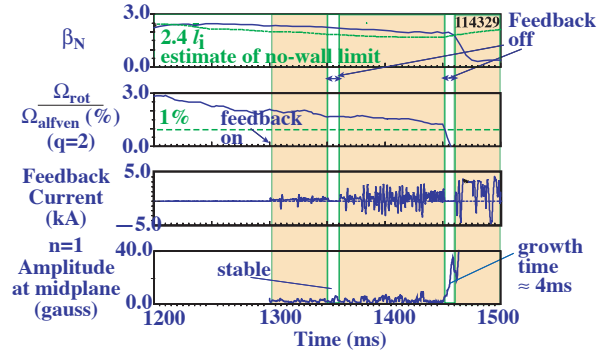


FIG. 4. The RWM onset with pulsed gating of the magnetic feedback: (a) β_N , (b) plasma rotation relative to the Alfvén velocity, (c) a feedback coil current (IU30), and (d) the $n=1$ δB_p amplitude.

4. Direct Magnetic Feedback RWM Stabilization at $\Omega_{rot} < \Omega_{crit}$

Direct magnetic feedback control with the I-coils is expected to be the primary means for maintaining stability well below the critical rotation angular frequency Ω_{crit} . The magnetic feedback stabilization has been investigated with 3 approaches: (1) gating off the feedback at low plasma rotation, (2) producing the near-zero rotation condition with active $n=1$ resonant braking and (3) exploring high C_β at lower rotation in comparison with Ω_{crit} predicted by MARS-F.

4.1. Direct Magnetic Feedback Study

A demonstration of direct feedback as shown by gating off the feedback is seen in the same discharge that was discussed in Section 3.2 (Fig. 4). The plasma discharge was maintained after the feedback was gated off at $t=1350$ ms but, the plasma rotation was gradually decreased presumably due to the viscous damping by the small, but non-zero, amplitude of RWM activity. When the feedback was turned off again at 1450 ms at reduced rotation level $\Omega_{rot}/\Omega_A = 1.2\%-1.3\%$, the $n=1$ amplitude increased rapidly with the growth time of 4 ms and the amplitude reached 30 G. When feedback was resumed 10 ms later, the discharge could not be recovered simply due to the large mode amplitude. These results indicate that the critical plasma rotation Ω_{rot}/Ω_A is around $1.3\%-1.7\%$ and that below this critical value magnetic feedback stabilization is required to maintain the discharge.

Another study of direct feedback control stabilization was the use of a near-zero rotation plasma produced by applying magnetic braking resonant on the $n=1$ RWM structure. Figure 5 shows a case where strong magnetic braking reduced the plasma rotation to essentially zero, over the outer half of the minor radius, where all of the $n=1$ rational surfaces are located. With I-coil feedback control, this discharge survives for >100 ms after the rotation is reduced. A discharge without feedback becomes unstable even with higher rotation and lower β .

4.2. Higher C_β Achievement at Lower Plasma Rotation

Higher C_β can be achieved at lower plasma rotation using I-coils. Achievable C_β is summarized with representative shot trajectories vs. rotation at the $q \approx 2$ surface as shown in Fig. 6. All trajectories are from discharges similar to the one shown in Fig. 4. These traces are all with I-coils except the one marked with C-coil and the one with no feedback. The marginal stabilization critical boundary in the absence of feedback using MARS-F code is shown by the dotted line. The marginal stability criterion is typical for this type of discharge condition, not for a specific shot, and qualitatively describes the marginal stability. Without feedback, a discharge is terminated below the estimated critical rotation [trajectory (a)]. With

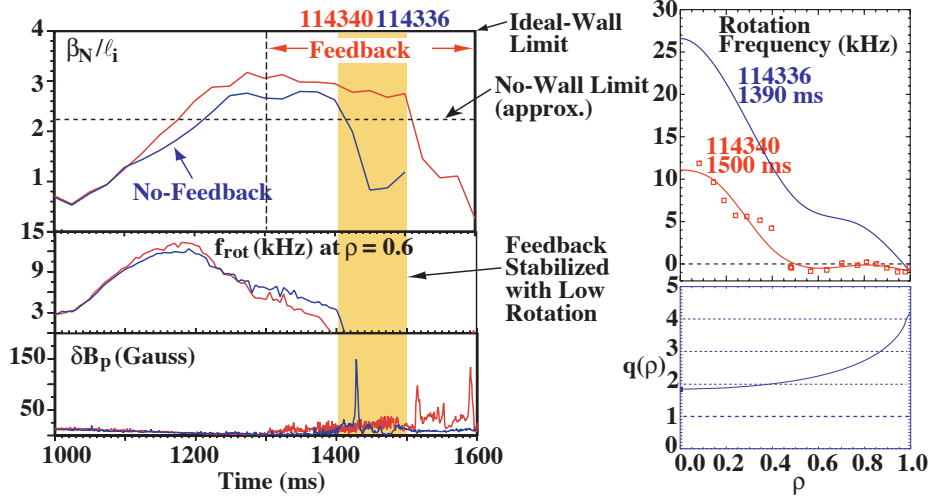


FIG. 5. Feedback stabilizes the RWM with the plasma rotation reduced to nearly zero over the outer half minor radius by $n=1$ resonant braking (red curves). A comparison case without feedback is unstable even with higher rotation and lower beta (blue curves). (Plasma velocity is measured by change exchange recombination light of impurity ions.)

feedback a proper choice of gains increased the plasma beta to $C_\beta \geq 0.8$, [trajectories (b1), (b2)], even when the plasma rotation is gradually reduced well below the predicted critical rotation. The trace (b1) was terminated by a fast RWM. The shot (b2) reached higher C_β with even lower rotation (30 km/s, kink with the growth time of 100–150 μ s at corresponding to $\approx 0.4\%$ of Ω_A) and was terminated by a fast growing 10 kHz oscillation, at which frequency the wall should act as an ideal wall. With external C-coils, such high C_β was not achieved with reduced rotation level such as $\Omega_{rot}/\Omega_A \leq 0.5\%$. The excitation of such a fast growing oscillatory mode indicates the stability condition is approaching to the ideal kink branch. A trajectory of the best performance with C-coil feedback is included for comparison [trajectory (d)]. I-coil feedback produced higher plasma pressure when compared to the C-coils even when the plasma rotation was significantly reduced. The plasma rotation with nearly zero by resonant $n=1$ magnetic braking discussed in the previous subsection is shown by a trajectory (c). Feedback with the I-coils can sustain the plasma at $\approx 40\%$ above no-wall limit, $C_\beta \approx 0.4$, for > 100 ms. The range of $C_\beta \approx 0.4$ – 0.5 is consistent with both MARS-F and VALEN predictions for non-rotating plasma due to the present power supply time characteristics (which are based on the measured power supply response) [9].

The open loop growth rates of various shots can be determined when rapid RWM growth takes place at the highest beta limit near termination of a discharge and the feedback system has exhausted the available current. At that moment, the plasma rotation is reduced to nearly zero due to the strong viscous effect of an uncontrolled RWM and the observed growth rate should correspond to that without any stabilization. The observed growth rates are in good agreement with model predictions. The solid line is the growth rate calculated by VALEN without feedback as shown in Fig. 7. The result suggests that the feedback system with I-coils can suppress the RWM growth rate up to $\gamma\tau_w > 10$ with some plasma rotation.

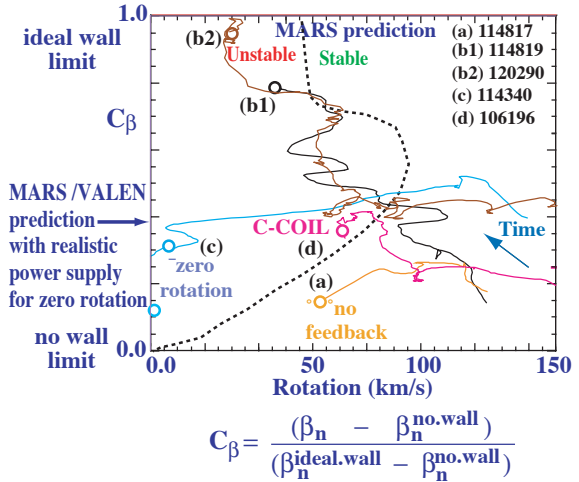


FIG. 6. Discharge trajectories, (a) no-feedback, (b) high C_β , (c) zero rotation with $n=1$ resonant braking, and (d) with C-coils.

5. MARS Analysis

An MHD analysis code, MARS-F [10], using measured profiles has been demonstrated as a useful tool for examining rotational as well as direct magnetic feedback stabilization of the RWM. The MARS code also includes the realistic geometry of the vacuum vessel, the internal feedback coils and feedback sensors. Based on the high C_β shot (114819: the trace of (b1) in Fig. 6), a series of equilibria were prepared for the stability analysis (here we report cases with $C_\beta = 0.4$ and 0.8). The sound wave damping model is used with the damping strength parameter of $\kappa_{||} = 0.5$ [18]. Since the MARS-F code predicts the wall time constant to be 2.5 ms, in the following discussion we use this value as τ_w^* and the normalized growth rate $\gamma\tau_w^*$ is a useful measure to be compared with experiments and other code results. The gain G^* in MARS-F code is not normalized.

5.1. The Critical Rotation Velocity

The growth time with rotation from MARS-F is consistent with the experiment. Figure 8 shows the RWM complex growth rate for $C_\beta = 0.4$ and its sensitivity to the plasma rotation with fixed normalized rotation profile. The normalized growth rate $\gamma\tau_w^*$ without rotation ≈ 3.0 is consistent with VALEN predictions for $\gamma\tau_w$ with $C_\beta \approx 0.4$ (Fig. 2). The experimental rotation is about 85% of the critical rotation of $\Omega_{crit}/\Omega_A \approx 2.5\%$ at $q = 2$ surface. With the experimental rotation value, the growth rate, $\text{Re}(\gamma\tau_w^*) \approx 1.5$, is similar to the growth rate that was observed with the feedback turned-off during the experiment (Fig. 4). The imaginary part shows large discrepancy between the observed near-zero rotation frequency and the value of $\text{Im}(\gamma\tau_w^*) = 4-5$ predicted by MARS-F. This could be due the effect of residual error field influencing the onset near the marginally unstable condition. The growth rate $\gamma\tau_w^*$ is a steep function of rotation when Ω_{rot} is near Ω_{crit} and with even a slight variation in plasma rotation, the RWM mode growth time can either become stable or get closer to the value of growth time without the rotation. Since a slight change of profiles can easily occur during the course of discharge, the present apparent consistency should be considered as a qualitative guidance.

5.2. The Feedback Performance at $C_\beta \approx 0.4$

The overall feedback process with plasma rotation has been modeled using the MARS-F analysis. The MARS-F code [10] characterizes the plasma response with a rational transfer function. It was found that a transfer function of two poles and one zero is adequate to describe the plasma response. A pole with positive real part ($\gamma\tau_w^*$) represents the unstable RWM with no feedback and the zero with the negative real part ($\gamma\tau_w^*$) is strongly influenced by the sensor characteristics. Another pole with negative real part ($\gamma\tau_w^*$) may be related to the second stable eigenmode. The complete model incorporates the digital control systems's transfer function with proportional (G_p) and derivative (G_d) gain: $[G_p + G_d s\tau_d / (1 + s\tau_d)]$, $(1 + s\tau_p)$ the digitization sampling time of 90 μs , and the measured characteristics of the power supply expressed in terms of two poles [9]. Both time constants, τ_p and τ_d were set at

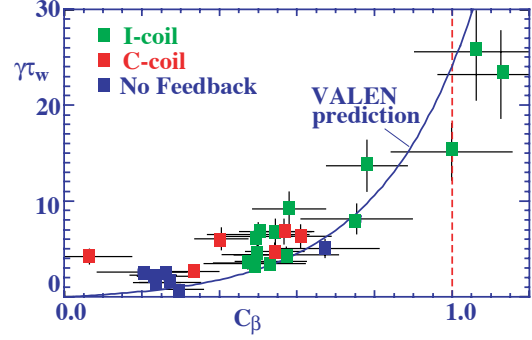


FIG. 7. The open loop RWM growth rate after feedback coil current saturation.

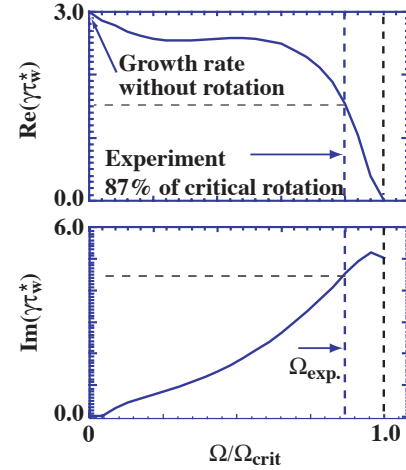


FIG. 8. MARS-F results: complex growth rate versus plasma rotation.

400 μs for most experiments. The dominant factor of the power supply is the delay time of 300 μs , primarily due to the 3.5 kHz switching frequency.

The predicted operational gain limits with the present hardware arrangement are limited as shown by the feedback stability dependence on gain in Fig. 9. With an increase in gain, the unstable plasma branch becomes less unstable and finally enters into the stable regime at $G = G_1$. On the other hand, the stable RWM branch becomes less stable and finally becomes unstable at $G = G_2$. (Also shown is a stable pole related to the time constant τ_p of the control algorithm.) The stable window is for gains such that $G_1 < G < G_2$. The high gain limit G_2 is only 70% above the minimum stable gain G_1 . The narrowness of the gain range is consistent with experimental results, where the system is stable with the gain varying by a factor of 2-3.

5.3. Power Supply Characteristics for High C_β

Further analysis of the stability of the feedback system shows that stabilization of the RWM requires the characteristic times of the control system to be short compared to the mode growth time. In this model, the power supply transfer function is represented by $\exp(-\tau_{\text{delay}}s)/(1 + s\tau_{\text{band}})$. Here s is the Laplace transform variable; τ_{band} and τ_{delay} characterize the total system bandwidth and the total system delay time. Figure 10 summarizes the results for the stability analysis of the stable operation window. The case chosen here is one near the operational limit of #114819 with $C_\beta = 0.8$ (a trajectory (b1) in Fig. 6) with 20% reduction of the plasma rotation from the experimental value to make the plasma slightly more unstable. With these parameter settings, the MARS-F predicts 600 μs growth time. The lower limit of gain is due to the minimum gain required to bring the unstable RWM into the stable regime [the G_1^* equivalent in Fig. 9] and the higher gain limit is due to the stable plasma pole going out into the unstable regime [G_2^* equivalent in Fig. 9]. The stability results show that power supply characteristic times must be a fraction (0.2–0.4) of the RWM growth time and the bandwidth and the delay time have to be balanced in a stringent manner. This may not be unreasonable, if we consider that feedback has to suppress the unstable mode within one growth time of when the mode starts to grow.

The present power supply of 3.5 kHz switching frequency causes a fixed 300 μs time delay and the digital plasma control system (PCS) of 90 μs -sampling rate presets the maximum bandwidth. The MARS result shown in Fig. 10 indicates that for $C_\beta = 0.8$ with 600 μs mode growth time, the present hardware combination of the delay time [(300+90) μs /600 μs \approx 0.7] and the bandwidth (90 μs /600 μs \approx 0.15) is not adequate for pursuing the RWM stabilization at high C_β . Currently upgrades to the power supply with audio amplifiers and improvement to the PCS are in progress.

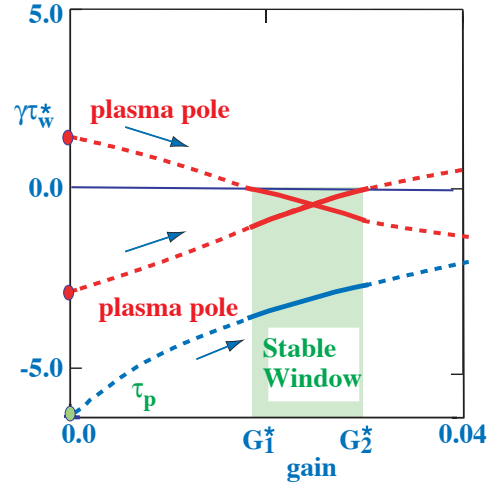


FIG. 9. MARS-F results: stability of several poles of the feedback equation, with $C_\beta = 0.4$.

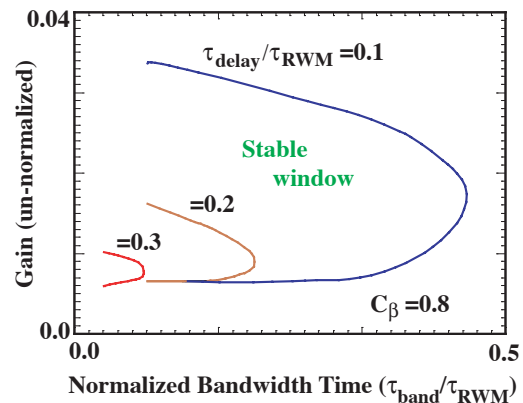


FIG. 10. MARS-F results: the stable gain window for conceptual power supply with $C_\beta = 0.8$. The gain is unnormalized.

6. Discussion

Application of RWM control feedback to the advanced tokamak is our ultimate goal. Figure 11 shows an example of near steady state high β_N discharge with and without RWM feedback. Without feedback, $n=1$ activity 20–30 G was excited at $t=1550$ ms leading to the β_N collapse. With feedback, the coil current amplitude of < 0.5 kA is sufficient to reduce the $n=1$ activity until a neoclassical tearing mode was excited around 2700 ms. The discharge was well over the estimated no-wall β_N limit and sustained for more than 1 s.

Internal I-coil feedback has successfully demonstrated the achievement of $C_\beta \approx 0.9$ at low rotation $\Omega_{rot}/\Omega_A < 1\%–2\%$, which is below the critical rotation Ω_{crit} estimated by MARS-F using the experimental profiles. The sustainment of $C_\beta \approx 0.3–0.4$ without plasma rotation over many wall time up to the theoretical C_β limit supports the fundamental advantage for direct magnetic feedback with internal I-coils, which was not observed with the previous use of the external C-coils. The internal I-coils are also more effective and efficient than external C-coils with less total coil current and with reduced amplitude of unnecessary non-resonant field components.

Now various MHD codes have been used to assess the stabilization status. The VALEN, NMA and MARS-F codes agree with the experimental observations such as the poloidal structure optimization, the open loop growth rate, and the feedback performance without plasma rotation. The MARS-F analysis of the feedback performance is also consistent with experimental observations. MARS-F predicts the power supply must have a fast response time, a fraction of the mode growth time. Feedback has sustained $\beta_N \approx 4$ advanced tokamak regime over 1 s.

Acknowledgment

Work supported by U.S. Department of Energy under DE-AC02-76CH03073, DE-FC02-04ER54698, W-7405-ENG-48, DE-FG02-89ER53297, DE-FG02-03ER83657, and DE-FG03-99ER82791.

References

- [1] KESSEL, C., *et al.*, Phys. Rev. Lett. **72**, 1212 (1994), 16; TURNBULL, A.D., *et al.*, Phys. Rev. Lett. **74** (1995) 718.
- [2] BONDESON, A. and WARD, D.J., Phys. Rev. Lett. **72**, 2709 (1994).
- [3] BISHOP C.M., Plasma Phys. Control. Fusion **31**, 1179 (1989).
- [4] BOOZER, A.H. Boozer, Phys. Plasmas **5**, 3350 (1998).
- [5] OKABAYASHI, M., *et al.*, Nucl. Fusion **38**, 1607 (1998).
- [6] LIU, Y.Q., BONDESON, A., *et al.*, Phys. Plasmas **7**, 3681 (2000).
- [7] BIALEK, J., *et al.*, Phys. Plasmas **8**, 2170 (2001).
- [8] OKABAYASHI, M., *et al.*, J. Plasma Fusion Res. SERIES, Vol. **5** (2002).
- [9] GAROFALO, A., JENSEN, T. H., and STRAIT, E.J., Phys. Plasmas **9**, 4573 (2002).
- [10] CHU, M.S., *et al.*, Phys. Plasmas **11**, 2497 (2004).
- [11] STRAIT, E.J., *et al.*, Nucl. Fusion **43**, 430 (2003).
- [12] OKABAYASHI, . *et al.*, Phys. Plasmas **8**, 2071 (2001),
- [13] GAROFALO, A. M., Phys. Plasmas **9**, 1997 (2002),
- [14] STRAIT, E.J., *et al.*, Phys. Plasmas **11**, 2505 (2004).
- [15] BOOZER, A.H., Rev. Letters **86**, 5059 (2001),
- [16] GAROFALO, A., Phys. Rev. Letters **89**, 235001 (2002),
- [17] REIMERDES, H., *et al.*, Phys. Rev. Letters **93** (2004) 135002.
- [18] CHU, M.S., *et al.*, Phys. Plasmas **2** (1995).
- [19] CHANCE, M.S., 30th EPS Conference on Controlled Fusion and Plasma Physics, St. Petersburg, Russia, July 7-11, 2003, P-2.109

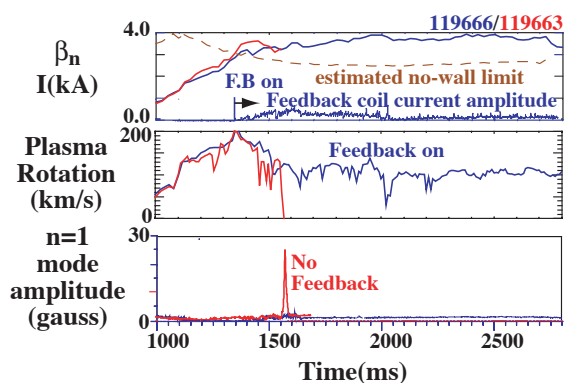


FIG. 11. Steady-state high β_N discharge with (blue) and without (red) RWM feedback.